

# Modelling and Analysis of Bidirectional DC-DC Converter

R. İlker Kayaalp, Tuğçe Demirdelen, Mehmet Tümay

Çukurova University, Department of Electrical and Electronics Engineering, Balcalı, Adana/TURKEY

[ikayaalp@cu.edu.tr](mailto:ikayaalp@cu.edu.tr), [tdemirdelen@cu.edu.tr](mailto:tdemirdelen@cu.edu.tr), [mtumay@cu.edu.tr](mailto:mtumay@cu.edu.tr)

## Abstract

*Bidirectional dc-dc converters are used lots of industrial areas such as electric vehicles, uninterruptable power supplies, fuel cells, solar panel cells as energy sources are searched in order to improve the quality of power at the transmission, distribution lines and other areas. The main contribution of this paper, applying the most common used control method on single phase isolated bidirectional full bridge dc-dc converter and comparing this control method (Extended Phase Shift – EPS) on efficiency way by with/without using snubber capacitors. In this paper, Isolated Bidirectional DC-DC Converter topology is modelled and controller algorithm is written by FORTRAN programming language. According to the results, it is observed that efficiency result of the converter, using snubber capacitors in the converter topology has higher performance than the snubberless system.*

## 1. Introduction

In recent years, different types of power hybrid electric vehicles, uninterruptable power supplies, fuel cells, solar panel cells as energy sources are searched in order to improve the quality of power at the transmission and distribution lines and other areas and those systems’ devices have been developed day by day. In these systems, for maximum efficiency in cases of charge and discharge via bi-directional voltage system between storage elements and direct current way require independent power sources. That's why bidirectional dc-dc converters between different dc sources provide energy exchanging and control mechanisms. These restrictions on the systems reveal importance of energy efficiency [1]. Thus, researchers design lots of different topologies and control methods for improving the converter system in literature.

Generally bi-directional dc-dc converters are isolated and non-isolated stand and they are divided into various topologies. Classification of DC-DC converters is shown in Figure 1.

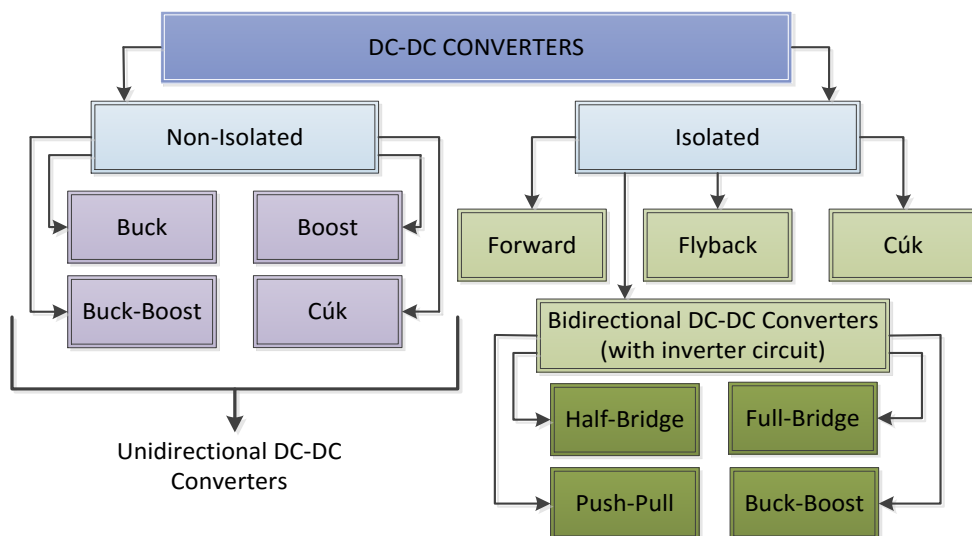


**Figure 1.** Classification of DC-DC Converters with Block Diagrams

In literature, different types of bidirectional isolated DC-DC converter topologies are studied by researchers. The most commonly used topology is full bridge, voltage source BDC topologies with high frequency isolation transformer [2][3]. This DC-DC converter provides zero voltage switching (ZVS) by using parasitic or external snubber capacitors to minimize losses. It can be used electric double layer capacitors and batteries. Thus, this topology usually preferred for various applications. Bidirectional isolated DC-DC converter based on a series resonant converter that has been considered as an interface between a low voltage bus (11-16 V) and a high voltage bus (220-447 V) in HEVs and EVs [4]. The drawback of the converter is that the series capacitor has to handle the full-load current, leading to increasing volume and cost. The current source (boost) full-bridge converter with an active-clamp snubber [5] and a passive clamp snubber [6] to fulfill high power, high current and a high voltage conversion ratio of a fuel-cell vehicle system. Moreover, the authors of [5] proposed the dc-link inductor should be placed at the low voltage battery side to improve the battery charging efficiency and minimize the ripple current. But, the low voltage side of the converter suffer from high transient voltage that necessitates the active or passive clamping snubbers.

In bidirectional DC-DC converter literature, lots of various control methods are tried for improving system efficiency. Generally, they use pulse width modulation (PWM) method and using control methods are single (traditional) phase shift (SPS) [7], extended phase shift (EPS) [8], dual phase shift (DPS) [9], triple phase shift (TPS) [10], PWM plus phase shift (PPS) [11], direct current slew rate control (DCSR) [12], sliding mode control (SMC) [13], phase-shifting shoot-through bivariate coordinated control (PSBCC) [14], etc...

On account of the limitations between existing literatures, the purpose of this paper is the following;

- 1) To improve the modelling of all system.
- 2) To implement the EPS control method on the snubberless system.
- 3) To implement the EPS control method on the system with snubber capacitors.
- 4) To compare efficiencies of the converter with/without snubber capacitors.

## **2. Modelling of Bidirectional DC-DC Converter**

Single-phase full-bridge bidirectional isolated buck-boost DC-DC converter topology (Figure 2) contains high frequency isolated transformer in order to provide smooth current flowing and the transformer is generally used 1:1. Therefore, 1:1 isolated transformer is used at this study. Totally 8 IGBTs are triggered by cosine signals. These signals can be different (1 or 0) according to control method algorithm that is created to fulfill the working necessities. Moreover, conditions of switches are represented by power flow ways. For PF1: A<sub>1</sub> and B<sub>2</sub> are ON, A<sub>2</sub> and B<sub>1</sub> are OFF. For PF2: A<sub>1</sub> and B<sub>2</sub> are OFF, A<sub>2</sub> and B<sub>1</sub> are ON. R<sub>1</sub>=R<sub>2</sub>=20ohm. In this paper, effect of snubber capacitors is investigated at the system by using EPS control method for buck and boost modes of the converter. The effect of the snubber capacitors decrease switching losses. Thus, performance value of the system is improved when the snubber capacitors are used in the BDC topology.

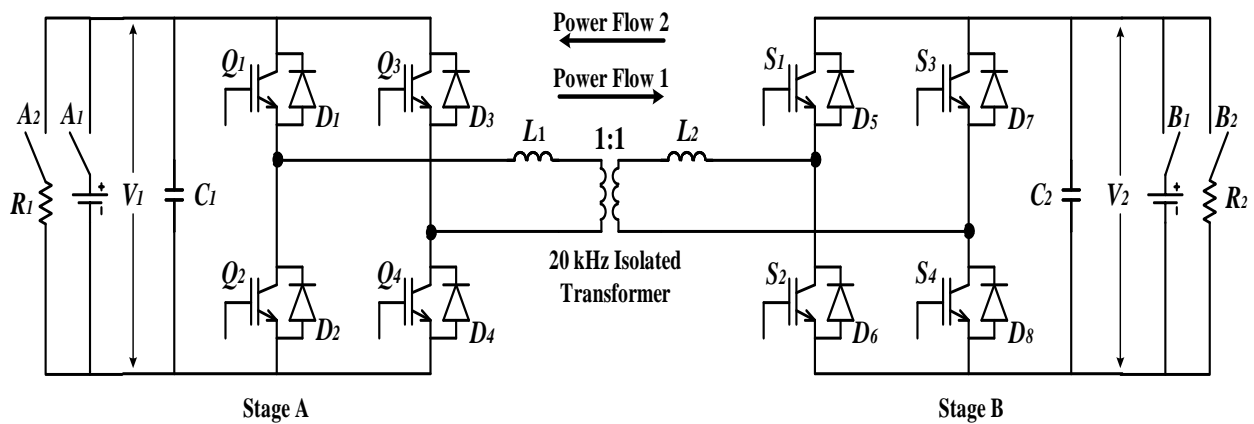


**Figure 2.** Circuit Topology of Single-Phase Full-Bridge Bidirectional Isolated Buck-Boost DC-DC Converter. Moreover, two inductors and two dc link capacitors are used at this circuit topology. Describing of inductors and capacitors is calculated as the below equations.

**2.1. Inductance Calculation**

The inductor design has a significant impact on a system performance, such as realization of complementary control ZVRT (Zero Voltage Resonant Transition) soft switching, device switching loss, system volume, inductor power loss, etc... It is necessary to optimize the inductance with all the design considerations.

The relationship between inductor peak current  $I_{peak}$ , minimum current  $I_{min}$ , and inductor RMS current  $I_{RMS}$  can be expressed in (1)-(5), where  $T_s$  is the switching period,  $I_{Load}$  is load current,  $P$  is the load power and  $\Delta I$  is the inductor current ripple.

$$\Delta I = \frac{1}{2} \cdot \frac{V_{in} - V_o}{L} \cdot \frac{V_o}{V_{in}} \cdot T_{sw} \tag{1}$$

$$I_{Load} = \frac{P}{V_o} \tag{2}$$

$$I_{peak} = I_{Load} + \Delta I \tag{3}$$

$$I_{min} = I_{Load} - \Delta I \tag{4}$$

$$I_{RMS} = \sqrt{I_{Load}^2 + \frac{\Delta I^2}{3}} \tag{5}$$

There is a formula that is used in [15] for calculating input and output inductors with phase-shift angle.

$$P = \frac{V_1 V_2 N}{\omega L} \times \left( \frac{\delta(\pi - \delta)}{\pi} \right) \tag{6}$$

Where;  $V_1$  and  $V_2$  are input and output voltages while considering buck and boost modes,  $N$  is high frequency transformer turn ratio,  $L$  is sum of the transformer leakage inductance and auxiliary inductor,  $\delta$  is a phase shift angle and finally  $w$  is equal to  $2\pi f$ .

Using the below equation for calculating inductors at buck and boost modes;

$$L = L_{Trans} + 2L_{Auxiliary} = \frac{V_1 V_2 N \times (\delta(\pi - \delta))}{2 \cdot P \cdot f \cdot \pi^2} \tag{7}$$

**2.2.DC Link Capacitors Calculation**

Firstly, the basic capacitor equation which is known. Capacitor current,  $i_c$  can be expressed as capacitor value,  $C$  times derivative of the voltage across this capacitor,  $V_{cap}$ .

$$i_{cap} = C \frac{dV_{cap}}{dt} \tag{8}$$

Extracting the capacitance  $C$  can be calculated as;

$$C = \frac{i_{cap} dt}{dV_{cap}} \tag{9}$$

At equation (9)  $dV_{cap}$  is voltage ripple across the capacitor and it is known for a design. Generally, small capacitor values give rise to bigger voltage ripple and this bigger voltage ripples cause to transfer more harmonics at the ac side load. Therefore, both small capacitor and low harmonics to the load are necessary. Obviously, a contradiction occurs and designers should consider this condition.

However, the ripple voltage of the converter is generally determined and equations (10) and (11) can be used for buck and boost modes in order to calculate input and output capacitors. In this way, creating of two capacitor values is possible if it is used  $C_1=C_{input}$ ,  $C_2=C_{output}$  for buck mode and  $C_1=C_{output}$ ,  $C_2=C_{input}$  for boost mode.

Input capacitor ( $C_{input}$ ) and output capacitors ( $C_{output}$ ) are calculated as;

$$C_{input} = \frac{\Delta I_L T_{sw}}{8\Delta V_o} \tag{10}$$

$$C_{output} = \frac{I_0 D T_{sw}}{\Delta V_o} \tag{11}$$

**2.3.Effect of Snubber Capacitors**

Generally, larger capacitances cause to reduce turn-off losses, but it should reduce turn-on losses too. The present aim is reducing the total of turn-off and turn-on losses. The snubber design can be simply done with energy equation that is charge balance of  $Cv^2$  and  $1/2Li^2$  shown at (12) [16].

$$C \cdot v^2 = \frac{1}{2} \cdot L \cdot i^2 \tag{12}$$

Here  $v$  is capacitor voltage and  $i$  is inductor current.

This calculation can be done for small capacitance values or total elimination of snubber capacitors, which is good for power MOSFETs. But this charge balance is insufficient to minimize the switching loss for significant IGBT tail current. For this case, an experimental research was made to determine better snubber capacitors at turn-on and turn-off losses under hard and soft switching conditions [16].

In this study, five cases were tested experimentally for snubber capacitor optimization.  $0.14\mu F$ ,  $0.1\mu F$ ,  $0.068\mu F$ ,  $0.033\mu F$  and  $0F$  capacitors were tried. The prototype with  $0.068\mu F$  gave the best efficiency result. Figure 3 shows turn-on and turn-off energy vs. current with various capacitance values [16].

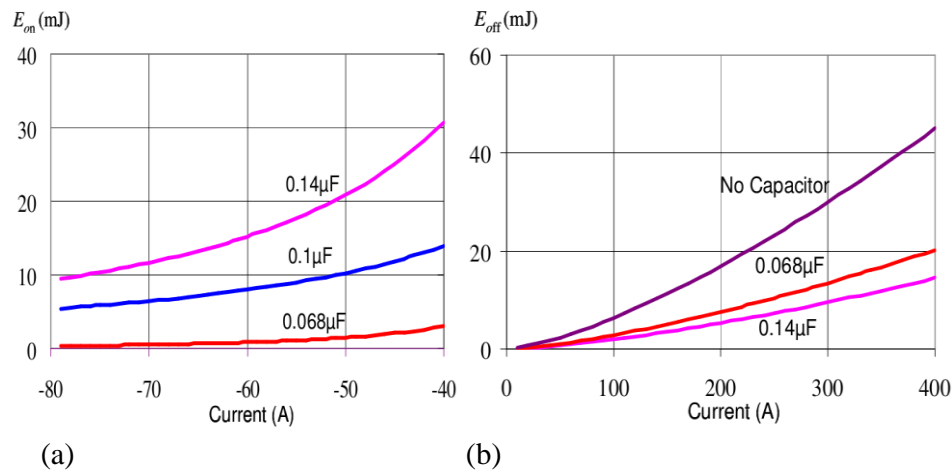


**Figure 3.** Turn-on and turn-off energy vs. current with various capacitance values

- (a) Turn-on energy vs. current
- (b) Turn-off energy vs. current

According to the above graphics, using the most efficient snubber capacitor ( $0.068\mu F$ ) affects 50% of the system performance. Therefore, if it is wanted to compare different phase shift control methods on efficiency, nonuse of snubber capacitors will be given better results at turn-off condition. In this way, this study measures efficiencies with or without using snubber capacitors.

### 3. Extended Phase Shift Control Method

In literature EPS control method is rarely used but more efficient than than single (traditional) phase shift control (SPS) and it is more applicable than dual phase shift control (DPS). Thus, EPS control is implemented for this system due to more feasible and provide high performance values. These researchers [8], [17], [18] used EPS control method in their studies.

EPS control method is operated by creating phase shift angles between Stage A and Stage B of the DC-DC converter in Figure 2. Moreover, one more phase shift angle should be defined between the one of the full bridges. It can be changeable to rectifier or inverter side. In short, there are two phase shift angles and first angle represents between of the S type IGBTs and Q type IGBTs. The other one can be represented between of the  $S_1$ - $S_2$  leg and  $S_3$ - $S_4$  leg or  $Q_1$ - $Q_2$  leg and  $Q_3$ - $Q_4$  leg. In this way, IGBTs are triggered with 1 or 0. Triggering signals are shown at Figure 4 and switching states (direction of current against minor time intervals) are demonstrated at Figure 5.

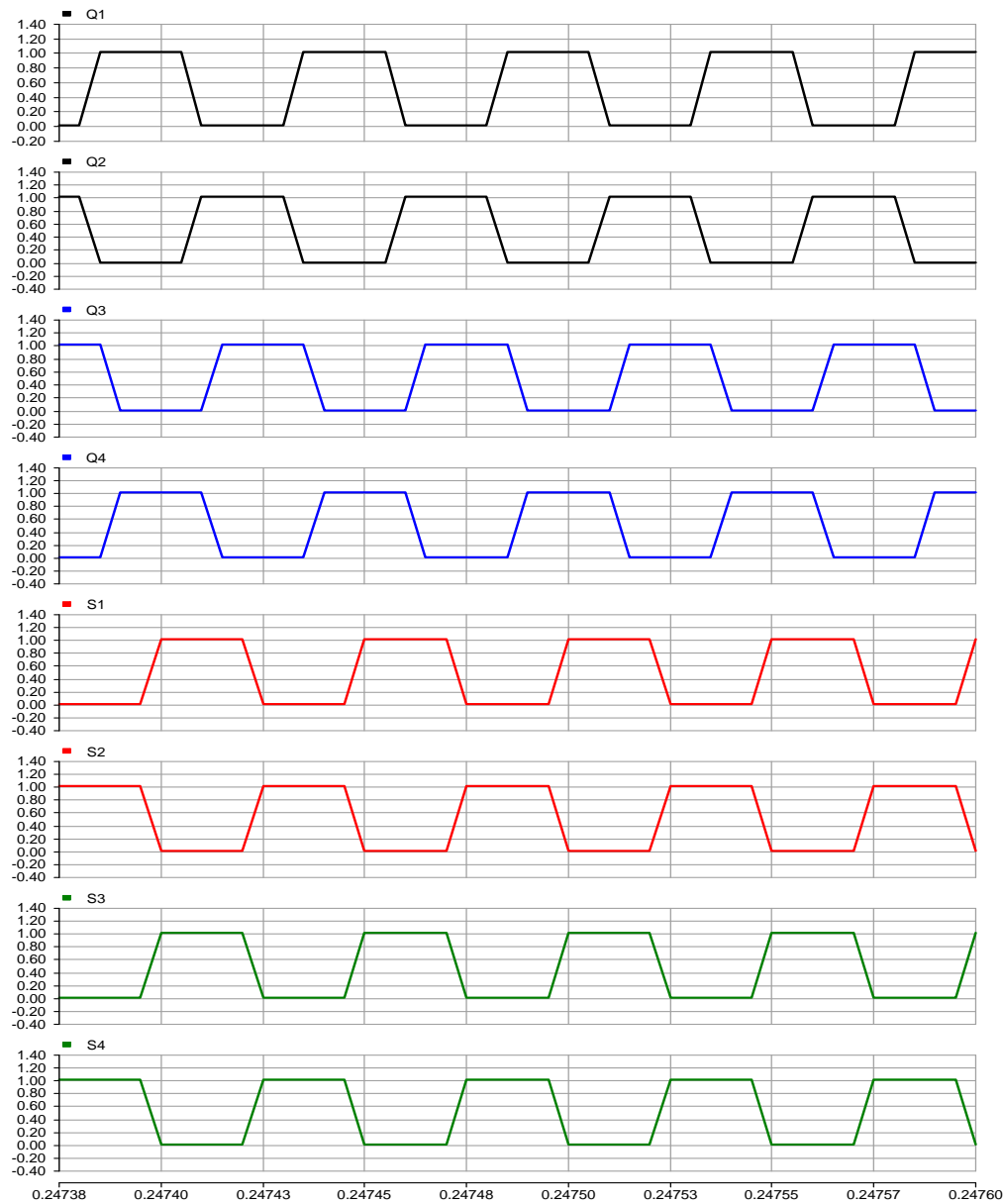
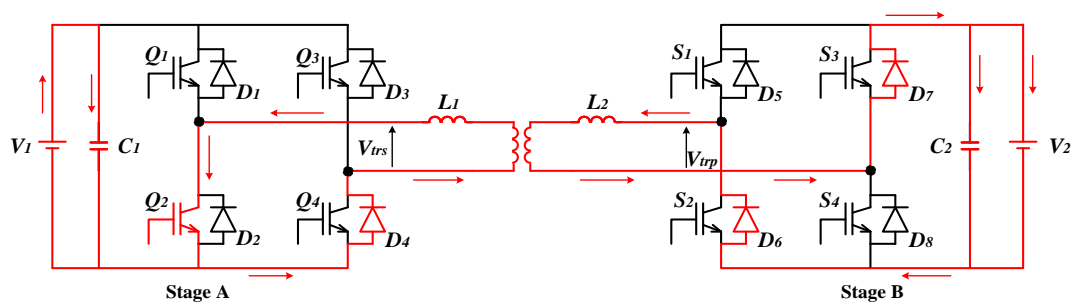
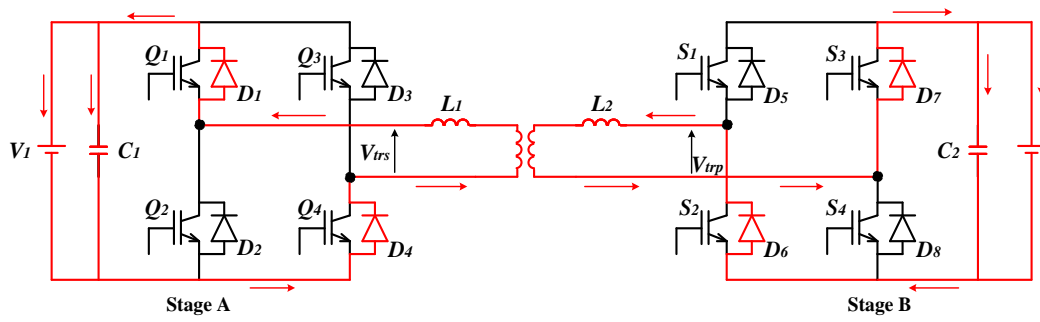


Figure 4. Triggers gate signals of EPS control method

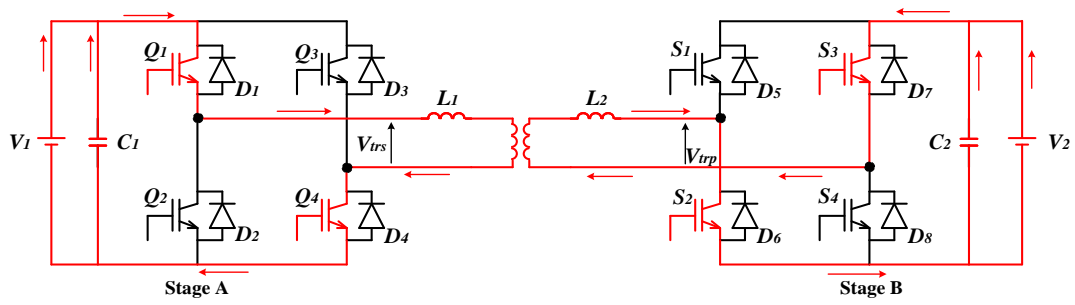
The switching cycle can be broken into 8 main intervals and operation modes are explained below the Figure 5 that shows switching states of EPS control.



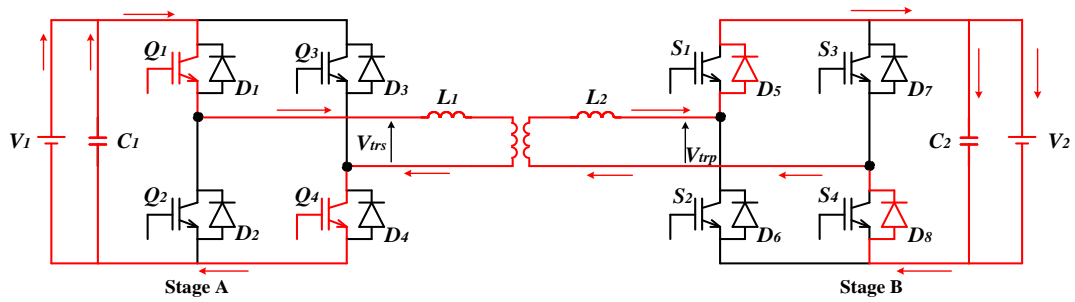
(a) Mode 1



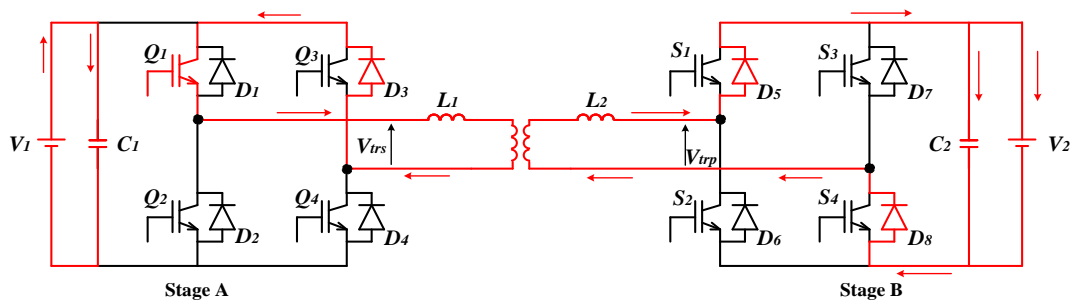
(b) Mode 2



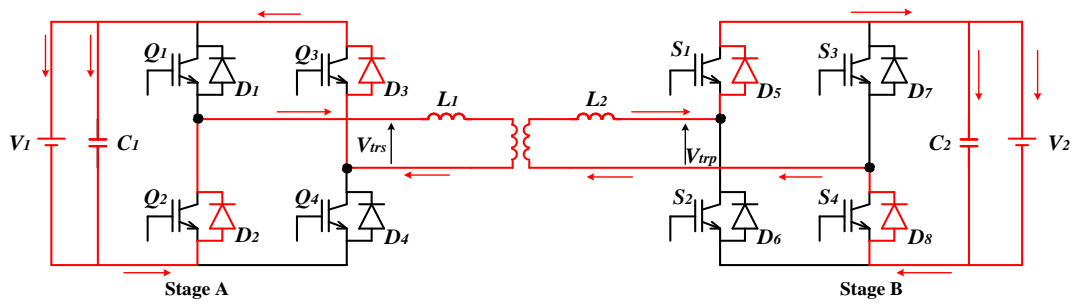
(c) Mode 3



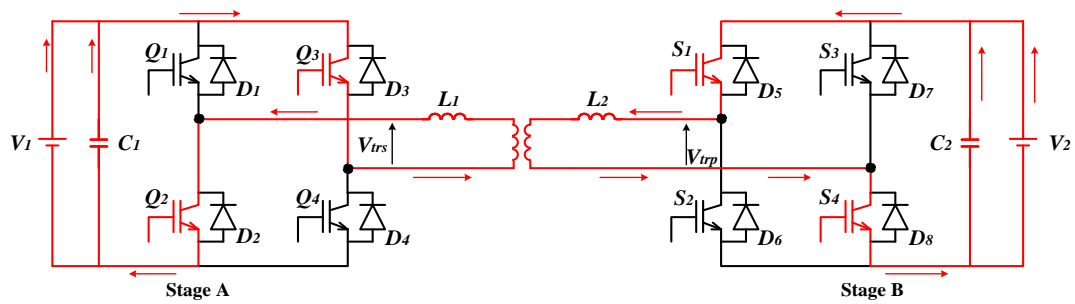
(d) Mode 4



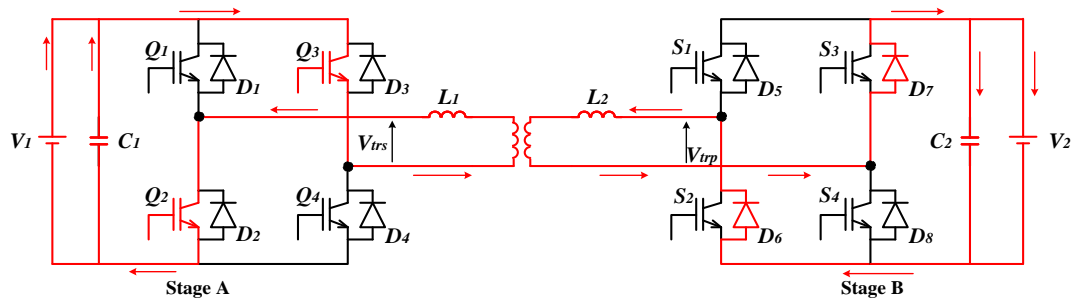
(e) Mode 5



(f) Mode 6



(g) Mode 7



(h) Mode 8

**Figure 5.** EPS Switching States Current Diagrams for Buck-Boost Modes [17]

These switching conditions are investigated for each time intervals and  $i_{L1}$  is calculated for them as shown below;

1) **Mode 1** ( $t_0 - t_1$ ):

$$i_{L1}(t) = i_{L1}(t_0) + \frac{nV_2}{L_1}(t - t_0) \tag{13}$$

2) **Mode 2** ( $t_1 - t_1'$ ):

$$i_{L1}(t) = i_{L1}(t_1) + \frac{V_1 + nV_2}{L_1}(t - t_1) \tag{14}$$

3) **Mode 3** ( $t_1' - t_2$ ):

$$i_{L1}(t) = i_{L1}(t_1) + \frac{V_1 + nV_2}{L_1}(t - t_1) \tag{15}$$

4) **Mode 4** ( $t_2 - t_3$ ):

$$i_{L1}(t) = i_{L1}(t_2) + \frac{V_1 - nV_2}{L_1}(t - t_2) \tag{16}$$

5) **Mode 5** ( $t_3 - t_4$ ):

$$i_{L1}(t) = i_{L1}(t_3) + \frac{-nV_2}{L_1}(t - t_3) \tag{17}$$

6) **Mode 6** ( $t_4 - t_4'$ ):

$$i_{L1}(t) = i_{L1}(t_4) + \frac{-V_1 - nV_2}{L_1}(t - t_4) \tag{18}$$

7) **Mode 7** ( $t_4' - t_5$ ):

$$i_{L1}(t) = i_{L1}(t_3) + \frac{-nV_2}{L_1}(t - t_3) \tag{19}$$

8) Mode 8 ( $t_4 - t_5$ ):

$$i_{L1}(t) = i_{L1}(t_5) + \frac{-V_1 + nV_2}{L_1} (t - t_5) \tag{20}$$

4. Simulation Cases and Results

Simulations are examined for the Table 1. Cases are changeable according to power flow way, buck-boost modes and parameters of circuit components. Representation of the measured values of the converter are defined in Figure 6.

Table 1. Cases of BDC with EPS Control Simulation; PF1: Power Flow 1, PF2: Power Flow 2

Converter Parameters			$V_1$	$V_2$	$C_1$	$C_2$	$L_1$	$L_2$	$n$	$f$
PF1	Buck	Case1	200V	160V	56mF	144mF	18μH	12μH	1:1	20kHz
PF2	Boost	Case2	160V	100V	56mF	144mF	18μH	12μH	1:1	20kHz

Single-Phase Full-Bridge Bidirectional Isolated Buck-Boost DC-DC Converter

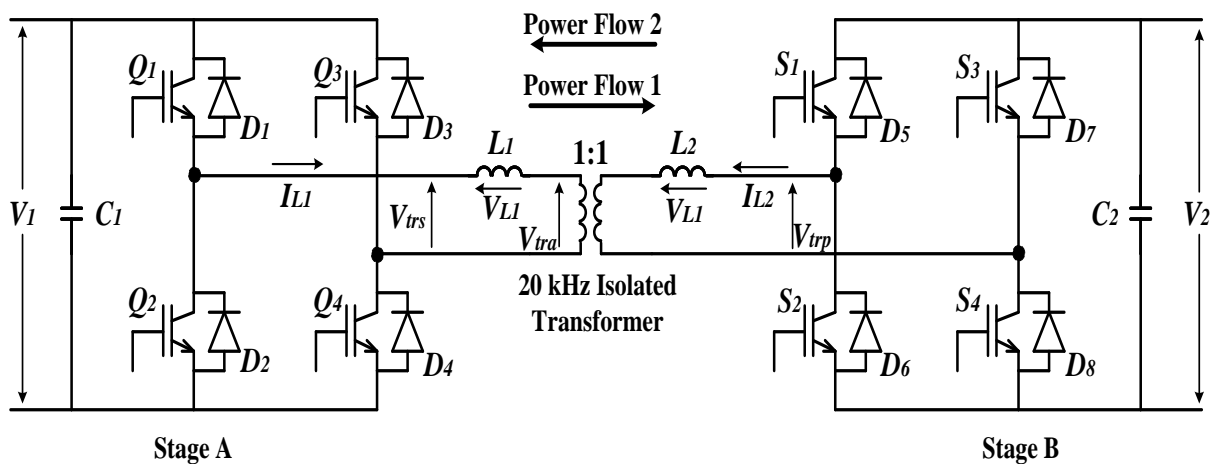


Figure 6. Measured values on the converter topology.

4.1. Simulation Results of Case 1

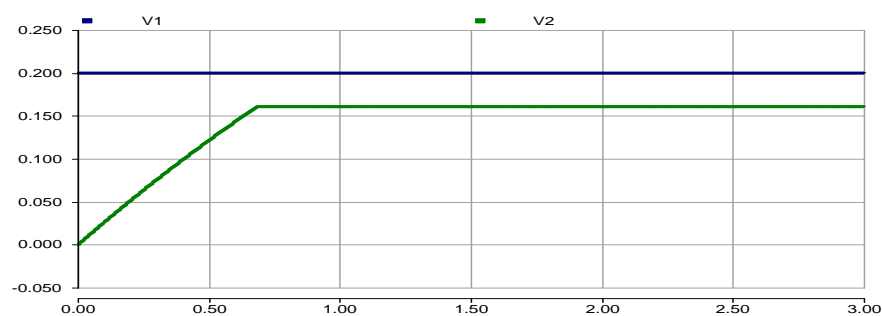


Figure 7. DC Link Voltages

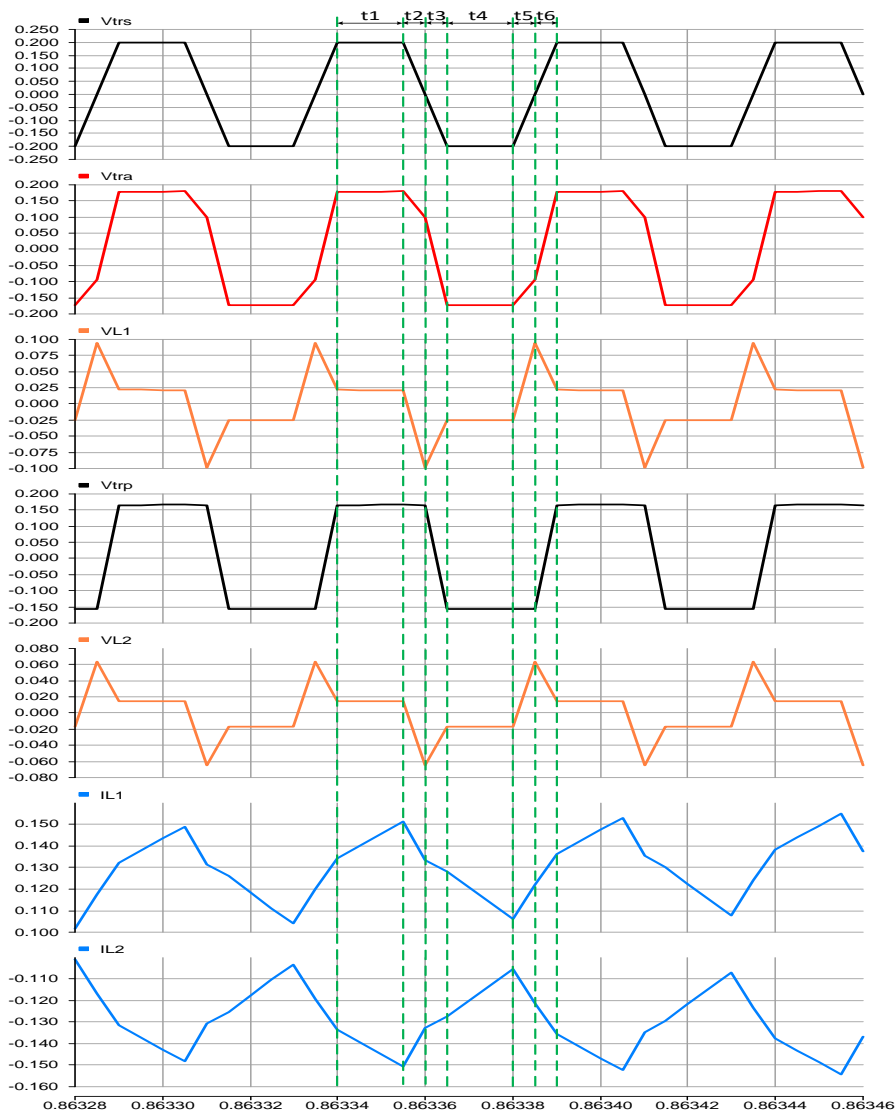


Figure 8. Voltage and Current Waveforms of Buck Mode at EPS Control

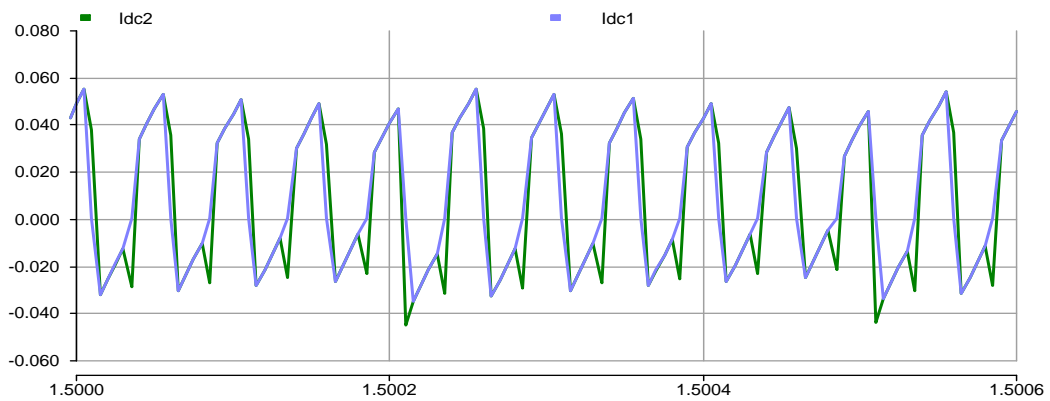


Figure 9. DC-Link Input and Output Currents

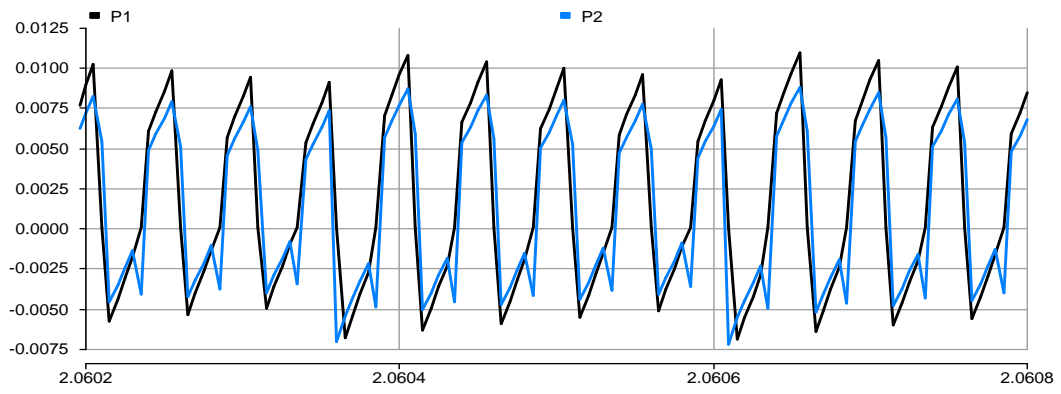


Figure 10. Input and Output Power Waveforms

#### 4.2. Simulation Results of Case 2

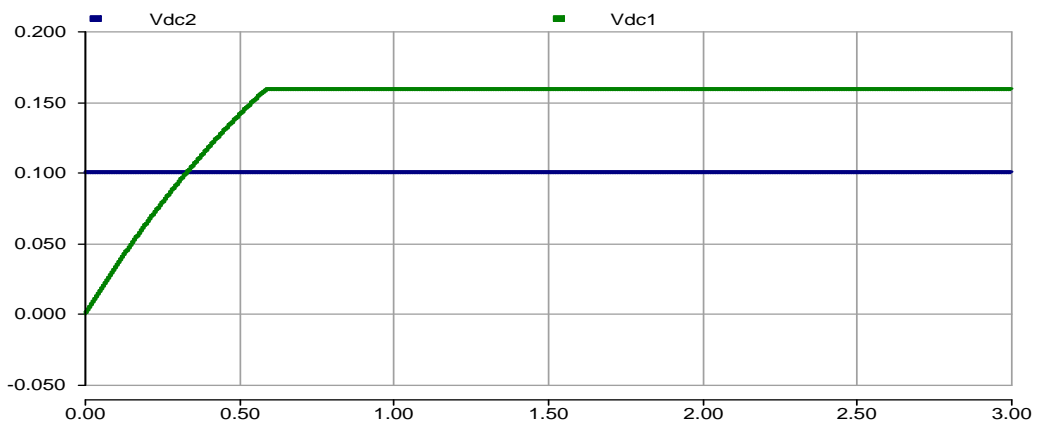


Figure 11. DC Link Voltages

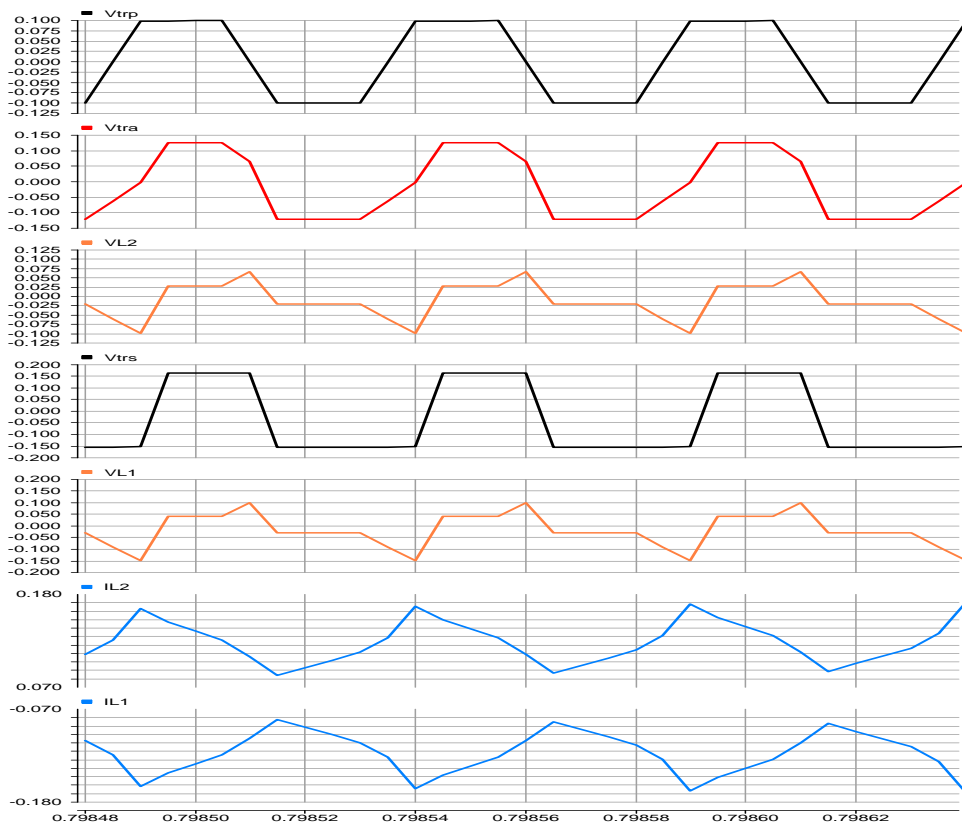


Figure 12. Voltage and Current Waveforms of Boost Mode at EPS Control

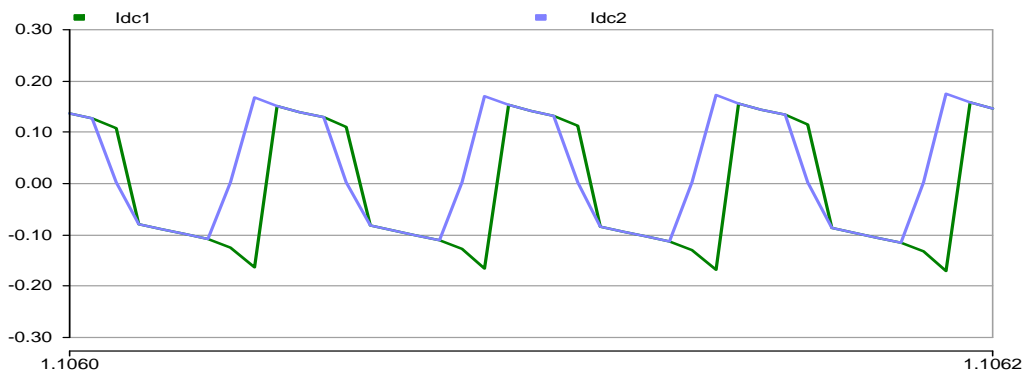


Figure 13. DC-Link Input and Output Currents

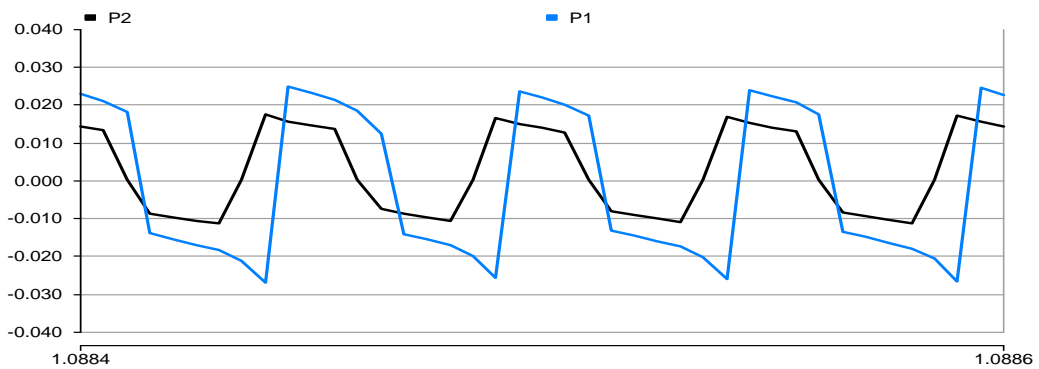


Figure 14. Input and Output Power Waveforms

All simulations 20Ω load resistance is used for both power flows. In Figure 7 and 11, DC-Link voltages of the BDC converter are given with settling time of the output voltage  $V_2$ . Voltage and current waveforms are triangular signals that provide easily observation of input and output transformer voltage waveforms. Especially, ( $V_{trs}=V_{tra}+V_{LI}$ ) this equation provides to make better comments about the Figure 8 and 12. Waveform of DC-link input and output currents are similar to input and output voltage waveforms of the converter at Figures 9-10-13-14. Additionally, these simulations are operated by same converter parameters with using 0.068μF snubber capacitors which are parallel connected to each IGBT and diode pairs. In this way, efficiency values of the converter are calculated for both snubberless and snubberly system by using the below equation.

$$\eta = \frac{P_{in} - (P_{in} - P_{out})}{P_{in}} \times 100 = \frac{P_{in} - P_{totalloss}}{P_{in}} \times 100 \tag{21}$$

### 5. Conclusion

Simulations are applied in PSCAD/EMTDC and voltage-current waveforms are validated with theoretical analysis. Firstly, this customization works beginning with finding of common used bidirectional DC-DC converter topology and control method. Secondly, calculation of converter parameters (capacitors, inductors, transformer windings) and calculation of phase shift angles for EPS control method are confirmed. Thirdly, simulations are operated and their results are compared with literature results. Therefore, simulation results are validated with theoretical analysis. Finally, power losses are calculated for EPS control method by benefiting from simulation results and efficiencies are obtained by using or without using snubber capacitors. Table 2 shows efficiency results of the BDC converter.

**Table 2.** Comparison of Efficiencies with/without using snubber capacitors at EPS Control.

	Power Flow	Operating Modes	Cases	$V_1$ - $V_2$	$f_{sw}$	EPS
Snubberless	1	Buck	Case 1	200V-160V	20kHz	78.5%
	2	Boost	Case 2	100V-160V	20kHz	61.2%
Using Snubbers	1	Buck	Case 1	200V-160V	20kHz	97.9%
	2	Boost	Case 2	100V-160V	20kHz	97.6%

Consequently, EPS control method is compared without using snubber capacitors by decreasing costs, while the rate of input and output voltages are not high and it is found that EPS can be preferred instead of DPS. EPS has more advantage than SPS and DPS in both feasibility way and mathematical complexity. In this way, the efficiency analysis of EPS control on the BDC topology with/without using snubber capacitors Thus, this condition emphasizes importance of the study.

### Acknowledgement

The authors would like to acknowledge the Scientific Research Project Unit of Cukurova University (Project Number: FYL-2014-3276)

## References

- [1] LEE S. –W., LEE S. –R., JEON C. -H., 2006. A New High Efficient Bidirectional DC/DC Converter in the Dual Voltage System, *Journal of Electrical Engineering & Technology*, Volume: 1, No: 3, Page(s): 343-350
- [2] DE DONCKER R. W., DIVAN D. M., KHERALUWALA M. H., 1991. A Three Phase Soft-Switched High-Power-Density DC-DC Converter for High Power Applications, *Industrial Applications, IEEE Transactions on*, Volume: 27, No: 1, Page(s): 63-73
- [3] KHERALUWALA M. H., GASCOIGNE R. W., DIVAN D. M., BAUMANN E. D., 1992. Performance Characterization of a High-Power Dual Active Bridge DC-to-DC Converter, *Industrial Applications, IEEE Transactions on*, Volume: 28, No: 6, Page(s): 1294-1301
- [4] KRISMER F., BIELA J., KOLAR J. W., 2005. A Comparative Evaluation of Isolated Bidirectional DC-DC Converters with Wide Input and Output Voltage, *Industrial Applications Conference, IEEE Transactions on*, Volume:1, Page(s): 599-606
- [5] WANG K., LIN C. Y., ZHU L., QU D., LEE F. C., LAI J., 1998. Bidirectional DC-to-DC Converters for Fuel Cell Systems, *Transportation, IEEE Workshop Power Electronics*, Page(s): 47-51
- [6] ZHU L., 2006. A Novel Soft-Commutating Isolated Boost Full-Bridge ZVS-PWM DC-DC Converter for Bidirectional High Power Applications, *Power Electronics, IEEE Transactions on*, Volume: 21, No: 2, Page(s): 422-429
- [7] ZHAO C., ROUND S. D., KOLAR J. W., 2010. Full Order Averaging Modelling of Zero-Voltage-Switching-Phase-Shift Bidirectional DC-DC Converters, *IET Power Electronics*, Volume: 3, No: 3, Page(s): 400-410
- [8] REDDY S. K. G., SWARUPA V., 2013. Extended Phase Shift Control of Isolated Bidirectional DC-DC Converter for Renewable Energy Sources Connected to Micro Grid, *International Journal of Advanced Research in Electrical, Electronics and Instrumentation Engineering*, Volume: 2, No: 8, Page(s): 3864-3872
- [9] BAI H., MI C., 2008. Eliminate Reactive Power and Increase System Efficiency of Isolated Bidirectional Dual-Active-Bridge DC-DC Converters using Novel Dual-Phase-Shift Control, *Power Electronics, IEEE Transactions on*, Volume: 23, No: 6, Page(s): 2905-2914
- [10] WU K., W. DE SILVA C., DUNFORD W. G., 2012. Stability Analysis of Isolated Bidirectional Dual Active Full Bridge DC-DC Converter with Tripe Phase Shift Control, *Power Electronics, IEEE Transactions on*, Volume: 27, No: 4, Page(s): 2007-2017
- [11] DEHONG X., CHUANHONG Z., HAIFENG F., 2004. A PWM Plus Phase-Shift Control Bidirectional DC-DC Converter, *Power Electronics, IEEE Transactions on*, Volume: 19, No: 3, Page(s): 666-675
- [12] LINGYU X., DESHANG S., HONGYU C., 2014. A ZVS Bidirectional Three-Level DC-DC Converter with Direct Current Slew Rate Control of Leakage Inductance, *Energy Conversion Congress and Exposition Conference, IEEE*, Page(s): 4410-4415
- [13] WANG J., LI S., YANG J., WU B., LI Q., 2015. Extended state observer-based sliding mode control for PWM based DC-DC buck power converter systems with mismatched disturbances, *IET Control Theory Applications*, Volume: 9, No: 4, Page(s): 579-586
- [14] ZHAO B., YU Q., LENG Z., CHEN X., 2012. Switched Z-Source Isolated Bidirectional DC-DC Converter and Its Phase-Shifting Shoot –Through Bivariate Coordinated Control Strategy, *Industrial Electronics, IEEE Transactions on*, Volume: 59, No: 12, Page(s): 4657-4670
- [15] INOUE S., AKAGI H., 2007. A Bidirectional DC-DC Converter for an Energy Storage System With Galvanic Isolation, *Power Electronics, IEEE Transactions on*, Volume: 22, No: 6, Page(s): 2299-2306
- [16] ZHANG J., 2008. Bidirectional DC-DC Power Converter Design Optimization, Modeling and Control, Doctor of Philosophy Thesis, Blacksburg-Virginia

- [17] ZHAO B., YU Q., SUN W., 2012. Extended-Phase-Shift Control of Isolated Bidirectional DC-DC Converter for Power Distribution in Microgrid, *Power Electronics, IEEE Transactions on*, Volume: 27, No: 11, Page(s): 4667-4680
- [18] SHI X., JIANG J., GUO X., 2013. An Efficiency-Optimized Isolated Bidirectional DC-DC Converter with Extended Power Range for Energy Storage Systems in Microgrids, *Open Access, Energies*, Volume: 6, Page(s): 27-44